RESEARCH ARTICLE

National Science Review
8: nwaa212, 2021
doi: 10.1093/nsr/nwaa212
Advance access publication 31 August 2020

PHYSICS

Finite-size scaling of O(n) systems at the upper critical dimensionality

Jian-Ping Lv[1,*], Wanwan Xu[1], Yanan Sun[1], Kun Chen[2,*] and Youjin Deng[3,4,*]

[1]Department of Physics, Anhui Key Laboratory of Optoelectric Materials Science and Technology, Key Laboratory of Functional Molecular Solids, Ministry of Education, Anhui Normal University, Wuhu 241000, China; [2]Department of Physics and Astronomy, Rutgers, The State University of New Jersey, Piscataway, NJ 08854-8019, USA; [3]National Laboratory for Physical Sciences at Microscale and Department of Modern Physics, University of Science and Technology of China, Hefei 230026, China and [4]Department of Physics and Electronic Information Engineering, Minjiang University, Fuzhou 350108, China

*Corresponding authors. E-mails: jplv2014@ahnu.edu.cn; chenkun0228@gmail.com; yjdeng@ustc.edu.cn

Received 25 April 2020; **Revised** 29 June 2020; **Accepted** 29 June 2020

ABSTRACT

Logarithmic finite-size scaling of the O(n) universality class at the upper critical dimensionality ($d_c = 4$) has a fundamental role in statistical and condensed-matter physics and important applications in various experimental systems. Here, we address this long-standing problem in the context of the n-vector model ($n = 1, 2, 3$) on periodic four-dimensional hypercubic lattices. We establish an explicit scaling form for the free-energy density, which simultaneously consists of a scaling term for the Gaussian fixed point and another term with multiplicative logarithmic corrections. In particular, we conjecture that the critical two-point correlation $g(r, L)$, with L the linear size, exhibits a two-length behavior: follows r^{2-d_c} governed by the Gaussian fixed point at shorter distances and enters a plateau at larger distances whose height decays as $L^{-d_c/2}(\ln L)^{\hat{p}}$ with $\hat{p} = 1/2$ a logarithmic correction exponent. Using extensive Monte Carlo simulations, we provide complementary evidence for the predictions through the finite-size scaling of observables, including the two-point correlation, the magnetic fluctuations at zero and nonzero Fourier modes and the Binder cumulant. Our work sheds light on the formulation of logarithmic finite-size scaling and has practical applications in experimental systems.

Keywords: critical phenomena, universality class, O(n) vector model, finite-size scaling

INTRODUCTION

The O(n) model of interacting vector spins is a much-applied model in condensed-matter physics and one of the most significant classes of lattice models in equilibrium statistical mechanics [1,2]. The Hamiltonian of the O(n) vector model is written as

$$\mathcal{H} = -\sum_{\langle \mathbf{r}\mathbf{r}' \rangle} \vec{S}_{\mathbf{r}} \cdot \vec{S}_{\mathbf{r}'}, \qquad (1)$$

where $\vec{S}_{\mathbf{r}}$ is an n-component isotropic spin with unit length and the summation runs over nearest neighbors. Prominent examples include the Ising ($n = 1$), XY ($n = 2$) and Heisenberg ($n = 3$) models of ferromagnetism, as well as the self-avoiding random walk ($n \to 0$) in polymer physics. Its experimental realization is now available for various n values in magnetic materials [3–7], superconducting arrays [8,9] and ultracold atomic systems [10,11].

Finite-size scaling (FSS) is an extensively utilized method for studying systems of continuous phase transitions [12], including the O(n) vector model (1). Near criticality, these systems are characterized by a diverging correlation length $\xi \propto t^{-\nu}$, where the parameter t measures the deviation from the critical point and ν is a critical exponent. For a finite box with linear size L, the standard FSS hypothesis assumes that ξ is bounded by the linear size L, and thus predicts that the singular part $f(t, h)$ of the free-energy density scales as

$$f(t, h) = L^{-d} \tilde{f}(tL^{y_t}, hL^{y_h}), \qquad (2)$$

where $\tilde{f}$ is a universal scaling function, t and h represent the thermal and magnetic scaling fields, and $y_t = 1/\nu$ and y_h are the corresponding thermal and magnetic renormalization exponents, respectively. Furthermore, the standard FSS theory hypothesizes that, at criticality, the spin-spin correlation function $g(r, L) \equiv \langle \vec{S}_0 \cdot \vec{S}_{\mathbf{r}} \rangle$ of distance r decays as

$$g(r, L) \asymp r^{-(d-2+\eta)} \tilde{g}(r/L), \qquad (3)$$

where η relates to y_h by the scaling relation $\eta = 2 + d - 2y_h$. From (2) and (3), the FSS of

various macroscopic physical quantities can be obtained. For instance, from the second derivative of $f(t, h)$ with respect to t or h, it follows that, at criticality, the specific heat behaves as $C \asymp L^{2y_t-d}$ and the magnetic susceptibility diverges as $\chi \asymp L^{2y_h-d}$. The FSS of χ can also be calculated by summing $g(r, L)$ over the system. Furthermore, the thermodynamic critical exponents can be obtained by the (hyper-)scaling relations. For instance, in the thermodynamic limit ($L \to \infty$), the specific heat and the magnetic susceptibility scale as $C \propto t^{-\alpha}$ and $\chi \propto t^{-\gamma}$, where the critical exponents are $\alpha = 2 - d/y_t$ and $\gamma = (2y_h - d)/y_t$.

The O(n) model exhibits an upper critical dimensionality $d_c = 4$ such that the thermodynamic scaling in higher dimensions $d > d_c$ are governed by the Gaussian fixed point, which has the critical exponents $\alpha = 0$ and $\gamma = 1$, etc. In the framework of the renormalization group, the renormalization exponents near the Gaussian fixed point are

$$y_t = 2 \quad \text{and} \quad y_h = 1 + d/2 \tag{4}$$

for $d > d_c$.

Accordingly, the standard FSS formulae (2) and (3) predict that the critical susceptibility diverges as $\chi \asymp L^{2y_h-d} = L^2$ for $d > d_c$. However, for the Ising model on 5D periodic hypercubes, χ was numerically observed to scale as $L \asymp L^{5/2}$ instead of L^2 [13–18]. The FSS for $d \geq d_c$ turns out to be surprisingly subtle and remains a topic of extensive controversy [13–21].

It was realized that, for $d > d_c$, the Gaussian exponents y_t and y_h in (4) can be renormalized by the leading irrelevant thermal field with exponent $y_u = 4 - d$ as [22–25]

$$y_t^* = y_t - \frac{y_u}{2} = \frac{d}{2} \quad \text{and} \quad y_h^* = y_h - \frac{y_u}{4} = \frac{3d}{4}, \tag{5}$$

and the FSS of the free-energy density $f(t, h)$ becomes

$$f(t, h) = L^{-d} \tilde{f}(tL^{y_t^*}, hL^{y_h^*}). \tag{6}$$

In this scenario of the dangerously irrelevant field, the FSS of the critical susceptibility becomes $\chi \asymp L^{2y_h^*-d} = L^{d/2}$, consistent with the numerical results [13–15,17,18]. It was further assumed that the scaling behavior of $g(r, L)$ is modified as [16]

$$g(r, L) \asymp r^{-(d-2+\eta_Q)} \tilde{g}(r/L) \tag{7}$$

with $\eta_Q = 2 - d/2$, such that the decay of $g(r, L)$ is no longer Gaussian-like. In the study of the 5D Ising model [13], a more subtle scenario was proposed that $g(r, L)$ decays as r^{-3} at short distances, gradually becomes $r^{-5/2}$ for large distances and has a crossover behavior in between. The introduction of η_Q was refuted by Wittmann and Young [15] as the magnetic fluctuations at nonzero Fourier mode $\mathbf{k} \neq 0$ scale as $\chi_{\mathbf{k}} \asymp L^2$ and underlined in [17], which revealed that the nonzero Fourier moments are governed by the Gaussian fixed point instead of being contaminated by the dangerously irrelevant field.

Using random-current and random-path representations [26–28], Papathanakos [19] conjectured that the scaling behavior of $g(r, L)$ has a two-length form as

$$g(r, L) \asymp \begin{cases} r^{-(d-2)}, & r \leq \mathcal{O}(L^{d/[2(d-2)]}), \\ L^{-d/2}, & r \geq \mathcal{O}(L^{d/[2(d-2)]}). \end{cases} \tag{8}$$

According to (8), the critical correlation function still exhibits a Gaussian-like decay, $g(r, L) \asymp r^{-(d-2)}$, up to a length scale $\xi_1 = L^{d/[2(d-2)]}$, and then enters an r-independent plateau whose height vanishes as $L^{-d/2}$. Since the length ξ_1 is vanishingly small compared to the linear size, $\xi_1/L \to 0$, the plateau effectively dominates the scaling behavior of $g(r, L)$ and the FSS of χ. The two-length scaling form (8) has been numerically confirmed for the 5D Ising model and self-avoiding random walk, with a geometric explanation based on the introduction of an unwrapped length on the torus [18]. It is also consistent with the rigorous calculations for the so-called random-length random-walk model [20]. It is noteworthy that the two-length scaling is able to explain both the FSS $\chi_0 \equiv \chi \asymp L^{5/2}$ for the susceptibility (the magnetic fluctuations at the zero Fourier mode) [14] and the FSS $\chi_{\mathbf{k}} \asymp L^2$ for the magnetic fluctuations at nonzero modes [15,17].

Combining all the existing numerical and (semi-)analytical insights [13–20], Y.D. and coworkers extended the scaling form (6) for the free energy to be [21]

$$f(t, h) = L^{-d} \tilde{f}_0(tL^{y_t}, hL^{y_h}) + L^{-d} \tilde{f}_1(tL^{y_t^*}, hL^{y_h^*}), \tag{9}$$

where (y_t, y_h) are the Gaussian exponents (4) and (y_t^*, y_h^*) are still given by (5). Conceptually, scaling formula (9) explicitly points out the coexistence of two sets of exponents (y_t, y_h) and (y_t^*, y_h^*), which was implied in previous studies [15,17,18,20]. Moreover, a simple perspective of understanding was provided [21] that the scaling term with $\tilde{f}_1$ can be regarded as corresponding to the FSS of the critical O(n) model on a finite complete

graph with $V = L^d$ vertices. As a consequence, the exponents (y_t^*, y_h^*) can be directly obtained from exact calculations of the complete-graph O(n) vector model, which also gives $y_t^* = d/2$ and $y_h^* = 3d/4$. From this correspondence, the plateau of $g(r, L)$ in (8) is in line with the FSS of the complete-graph correlation function $g_{i\neq j} \equiv \langle \vec{S}_i \cdot \vec{S}_j \rangle$, which also decays as $V^{-1/2} = L^{-d/2}$. Note that, as a counterpart of the complete-graph scaling function, the term with $\tilde{f}_1$ should not describe the FSS of quantities merely associated with r-dependent behaviors, including magnetic/energylike fluctuations at nonzero Fourier modes. Therefore, in comparison with (6), scaling formula (9) can give the FSS of a more exhaustive list of physical quantities. The following gives some examples at criticality.

(i) Let $\vec{\mathcal{M}} \equiv \sum_{\mathbf{r}} \vec{S}_{\mathbf{r}}$ specify the total magnetization of a spin configuration, and measure its ℓ moment as $M_\ell \equiv \langle |\vec{\mathcal{M}}|^\ell \rangle$. Equation (9) predicts that $M_\ell \sim L^{\ell y_h^*} + q L^{\ell y_h}$, with q a nonuniversal constant. In particular, the magnetic susceptibility $\chi_0 \equiv L^{-d} M_2 \asymp L^{d/2}[1 + \mathcal{O}(L^{(4-d)/2})]$, where the FSS from the Gaussian term $\tilde{f}_0$ is effectively a finite-size correction, but its existence is important in analyzing numerical data [21].

(ii) Let $\vec{\mathcal{M}}_{\mathbf{k}} \equiv \sum_{\mathbf{r}} \vec{S}_{\mathbf{r}} e^{i\mathbf{k}\cdot\mathbf{r}}$ specify the Fourier mode of magnetization with momentum $\mathbf{k} \neq 0$, and measure its ℓ moment as $M_{\ell,\mathbf{k}} \equiv \langle |\vec{\mathcal{M}}_{\mathbf{k}}|^\ell \rangle$. The magnetic fluctuations at $\mathbf{k} \neq 0$ behave as $\chi_{\mathbf{k}} \equiv L^{-d} M_{2,\mathbf{k}} \sim L^{2y_h - d} = L^2$. The behaviors of χ_0 and $\chi_{\mathbf{k}}$ have been confirmed for the 5D Ising model [15,17,18,20].

(iii) The Binder cumulant $Q \equiv \langle |\vec{\mathcal{M}}|^2 \rangle^2 / \langle |\vec{\mathcal{M}}|^4 \rangle$ should take the complete-graph value, as expected from the correspondence between the term with $\tilde{f}_1$ in (9) and the complete-graph FSS. For the Ising model, the complete-graph calculations give $Q = 4[\Gamma(3/4)/\Gamma(1/4)]^2 \approx 0.456\,947$, consistent with the 5D result in [13].

Analogously, the FSS behaviors of the energy density, its higher-order fluctuations and the ℓ-moment Fourier modes at $\mathbf{k} \neq 0$ can be derived from (9).

We expect that the FSS formulae (8) and (9) are valid not only for the O(n) vector model but also for generic systems of continuous phase transitions at $d > d_c$. An example is given for percolation that has $d_c = 6$. It was observed [29] that, at criticality, the probability distributions of the largest-cluster size follow the same scaling function for 7D periodic hypercubes and on the complete graph.

In this work, we focus on the FSS for the O(n) vector model at the upper critical dimensionality $d = d_c$. In this marginal case, it is known that multiplicative and additive logarithmic corrections would appear in the FSS. However, exploring these logarithmic corrections turns out to be notoriously hard. The challenge comes from the lack of analytical insights, the existence of slow finite-size corrections, as well as the unavailability of very large system sizes in simulations of high-dimensional systems.

For the O(n) vector model, establishing the precise FSS form at $d = d_c$ is not only of fundamental importance in statistical mechanics and condensed-matter physics, but also of practical relevance due to the direct experimental realizations of the model, particularly in three-dimensional quantum critical systems [3–6,10,11]. For instance, to explore the stability of Anderson–Higgs excitation modes in systems with continuous symmetry breaking ($n \geq 2$), a crucial theoretical question is whether or not the Gaussian r-dependent behavior $g(r) \asymp r^{-2}$ is modified by some multiplicative logarithmic corrections.

SUMMARY OF THE MAIN FINDINGS

At the upper critical dimensionality ($d_c = 4$) of the O(n) model, state-of-the-art applications of FSS are mostly restricted to a phenomenological scaling form proposed by Kenna [30] for the singular part of the free-energy density, which was extended from Aktekin's formula for the Ising model [31],

$$f(t, h) = L^{-4} \tilde{f}(tL^{y_t}(\ln L)^{\hat{y}_t}, hL^{y_h}(\ln L)^{\hat{y}_h}) \tag{10}$$

for $n \geq 0$ and $n \neq 4$, where the renormalization exponents $y_t = 2$ and $y_h = 3$ are given by (4). Furthermore, the renormalization-group calculations predicted the logarithmic-correction exponents as $\hat{y}_t = (4 - n)/(2n + 16)$ and $\hat{y}_h = 1/4$ [32,33]. The leading FSS of χ_0 is hence given by $\chi_0 \asymp L^2(\ln L)^{1/2}$, independent of n.

Motivated by recent progress in O(n) models for $d > d_c$ [15–21], we hereby propose that, at $d = d_c$, the scaling form (10) for the free energy should be revised as

$$f(t, h) = L^{-4} \tilde{f}_0(tL^{y_t}, hL^{y_h}) + L^{-4} \tilde{f}_1(tL^{y_t}(\ln L)^{\hat{y}_t}, hL^{y_h}(\ln L)^{\hat{y}_h}), \tag{11}$$

and the critical two-point correlation $g(r, L)$ behaves as

$$g(r, L) \asymp \begin{cases} r^{-2}, & r \leq \mathcal{O}(L/(\ln L)^{\hat{p}}), \\ L^{-2}(\ln L)^{\hat{p}}, & r \geq \mathcal{O}(L/(\ln L)^{\hat{p}}), \end{cases} \tag{12}$$

with $\hat{p} = 2\hat{y}_h = 1/2$. By (12), we explicitly point out that no multiplicative logarithmic correction appears in the r dependence of $g(r, L) \asymp r^{-2}$, which is still Gaussian-like. By contrast, the plateau for $r \geq \xi_1 \sim L/(\ln L)^{\hat{p}}$ is modified as $L^{-2}(\ln L)^{\hat{p}}$. In other words, along any direction of the periodic hypercube, we have $g(r, L) \asymp r^{-2} + vL^{-2}(\ln L)^{\hat{p}}$, with v a nonuniversal constant. The r^{-2} decay at shorter distances in (12) is consistent with analytical calculations for the 4D weakly self-avoiding random walk and the O(n) ϕ^4 model directly in the thermodynamic limit ($L \to \infty$) [34], which predict $g(r) \asymp r^{-2}(1 + \mathcal{O}(1/\ln r))$.

The roles of terms with $\tilde{f}_0$ and $\tilde{f}_1$ in (11) are analogous to those in (9). The former arises from the Gaussian fixed point, and the latter describes the 'background' contributions ($\mathbf{k} = 0$) for the FSS of macroscopic quantities. However, note that the term with $\tilde{f}_1$ can no longer be regarded as an exact counterpart of the FSS of the complete graph, due to the existence of multiplicative logarithmic corrections. By contrast, the exact complete-graph mechanism applies to the $\tilde{f}_1$ term in (9), where the logarithmic correction is absent and $\tilde{f}_1$ corresponds to the free energy of the standard complete-graph model. According to (11), the FSS of various macroscopic quantities at $d = d_c$ can be obtained as follows.

(i) The magnetization density $m \equiv L^{-d}\langle|\vec{\mathcal{M}}|\rangle \asymp L^{-1}(\ln L)^{\hat{y}_h}[1 + \mathcal{O}((\ln L)^{-\hat{y}_h})]$.

(ii) The magnetic susceptibility $\chi_0 \asymp L^2(\ln L)^{2\hat{y}_h}[1 + \mathcal{O}((\ln L)^{-2\hat{y}_h})]$.

(iii) The magnetic fluctuations at $\mathbf{k} \neq 0$ Fourier modes $\chi_{\mathbf{k}} \asymp L^2$.

(iv) The Binder cumulant Q may not take the exact complete-graph value, due to the multiplicative logarithmic correction. Some evidence was observed in a recent study by Y.D. and his coworkers for the self-avoiding random walk ($n = 0$) on 4D periodic hypercubes, in which the maximum system size is up to $L = 700$.

The FSS of the energy density, its higher-order fluctuations and the ℓ-moment Fourier modes at $\mathbf{k} \neq 0$ can be obtained.

In quantities like m and χ_0, the FSS from the Gaussian fixed point effectively plays the role of finite-size corrections. Nevertheless, we note that in the analysis of numerical data, it is important to include such scaling terms.

We remark that the FSS formulae (11) and (12) for $d = d_c$ are less generic than (8) and (9) for $d > d_c$. For the O(n) models, a multiplicative logarithmic correction is absent in the Gaussian r dependence of $g(r, L)$ in (12). Although the two length scales are possibly generic features of models with logarithmic finite-size corrections at upper critical dimensionality, multiplicative logarithmic corrections to the r dependence of $g(r, L)$ require case-by-case analyses. Equation (11) can be modified in some of these models, which include the percolation and spin-glass models in six dimensions.

We proceed to verify (11) and (12) using extensive Monte Carlo (MC) simulations of the O(n) vector model. Before giving the technical details, in Fig. 1 we present complementary evidence for (11) and (12) in the case of the critical 4D XY model. In Fig. 1(a) we show the extensive data of $g(r, L)$ for $16 \leq L \leq 80$, of which the largest system

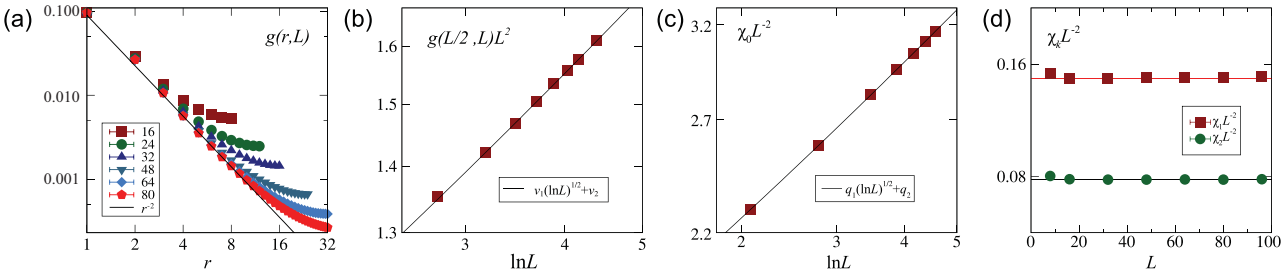

Figure 1. Evidence for conjectured formulae (11) and (12) in the example of the critical four-dimensional (4D) XY model. (a) Correlation function $g(r, L)$ on a log-log scale. The solid line denotes r^{-2} behavior. (b) Scaled correlation $g(r, L)L^2$ with $r = L/2$ versus ln$L$ on a log-log scale. Thus, the horizontal axis is effectively on a double logarithmic scale of L. The solid line represents logarithmic divergence with $\hat{p} = 1/2$. (c) Scaled magnetic susceptibility $\chi_0 L^{-2}$ versus ln$L$ on a log-log scale. The solid line accounts for logarithmic divergence with $\hat{p} = 1/2$. (d) Scaled $\mathbf{k} \neq 0$ magnetic fluctuations $\chi_1 L^{-2}$ and $\chi_2 L^{-2}$, with $\mathbf{k}_1 = (2\pi/L, 0, 0, 0)$ and $\mathbf{k}_2 = (2\pi/L, 2\pi/L, 0, 0)$, respectively. The horizontal lines strongly indicate the absence of logarithmic corrections in the scaling of $\chi_{\mathbf{k}}$.

contains about 4×10^7 lattice sites. To demonstrate the multiplicative logarithmic correction in the large-distance plateau indicated by (12), we plot $g(L/2, L)L^2$ versus $\ln L$ on a log-log scale in Fig. 1(b). The excellent agreement between the MC data and the formula $v_1(\ln L)^{1/2} + v_2$ provides a first piece of evidence for the presence of the logarithmic correction with exponent $\hat{p} = 1/2$. The second piece of evidence comes from Fig. 1(c), which suggests that the $\chi_0 L^{-2}$ data can be well described by the formula $q_1(\ln L)^{1/2} + q_2$. Finally, in Fig. 1(d) we plot the $\mathbf{k} \neq 0$ magnetic fluctuations χ_1 and χ_2 with $\mathbf{k}_1 = (2\pi/L, 0, 0, 0)$ and $\mathbf{k}_2 = (2\pi/L, 2\pi/L, 0, 0)$, respectively, which suppress the L-dependent plateau and show the r-dependent behavior of $g(r, L)$. Indeed, the $\chi_1 L^{-2}$ and $\chi_2 L^{-2}$ data converge rapidly to constants as L increases.

NUMERICAL RESULTS AND FINITE-SIZE SCALING ANALYSES

Using a cluster MC algorithm [35], we simulate Hamiltonian (1) on 4D hypercubic lattices up to $L_{\max} = 96$ (Ising, XY) and 56 (Heisenberg), and measure a variety of macroscopic quantities, including the magnetization density m, the susceptibility χ_0, the magnetic fluctuations χ_1 and χ_2 and the Binder cumulant Q. Moreover, we compute the two-point correlation function $g(r, L)$ for the XY model up to $L_{\max} = 80$ by means of a state-of-the-art worm MC algorithm [36].

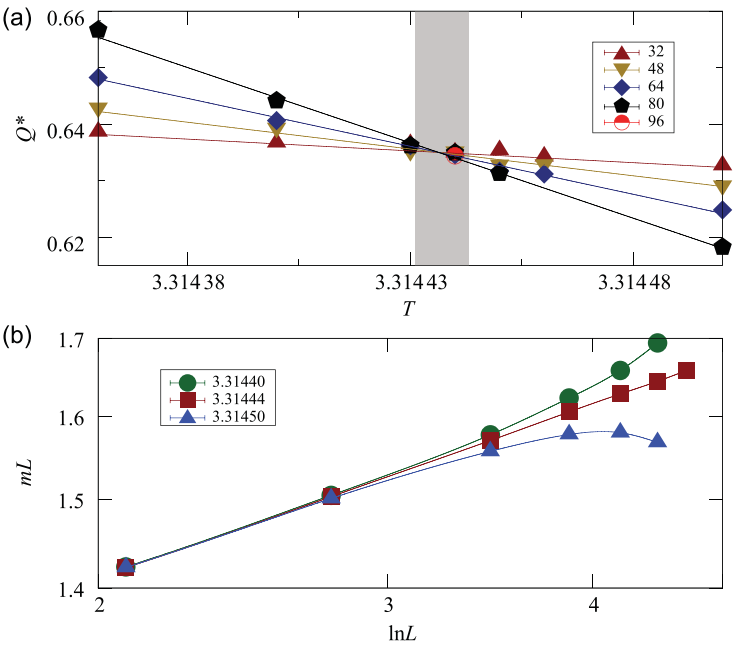

Figure 2. Locating T_c for the 4D XY model. (a) The Binder cumulant Q with finite-size corrections being subtracted, namely, $Q^*(L, T) = Q(L, T) - b(\ln L)^{-1/2}$, with $b \approx 0.1069$ according to a preferred least-squares fit. The shadow marks T_c and its error margin. (b) The magnetization density m rescaled by L^{-1} versus $\ln L$ around $T_c = 3.314\,44$ on a log-log scale.

Estimates of critical temperatures

In order to locate the critical temperatures T_c, we perform least-squares fits for the finite-size MC data of the Binder cumulant to

$$Q(L, T) = Q_c + atL^{y_t}(\ln L)^{\hat{y}_t} + b(\ln L)^{-\hat{p}} + c\frac{\ln(\ln L)}{\ln L}, \quad (13)$$

where t is explicitly defined as $T_c - T$, Q_c is a universal ratio, and a, b, c are nonuniversal parameters. In addition to the leading additive logarithmic correction, we include $c(\ln(\ln L))/\ln L$ proposed by Kenna [30] as a high-order correction, ensuring the stability of fits. In all fits, we justify the confidence in a standard manner: the fits with Chi squared (χ^2) per degree of freedom (DF) is $\mathcal{O}(1)$ and remains stable as the cutoff size $L_{\min}$ increases. The latter is a caution against possible high-order corrections not included. The details of the fits are presented in the online supplementary material.

By analyzing the finite-size correction $Q(L, T_c) - Q_c$, we find that the leading correction is nearly proportional to $(\ln L)^{-1/2}$, consistent with the prediction of (11) and (12). We let Q_c be free in the fits and have $Q_c = 0.45(1)$, close to the complete-graph result $Q_c = 0.456\,947$. Besides, we perform simulations for the XY and Heisenberg models on the complete graph and obtain $Q_c \approx 0.635$ and 0.728, respectively, also close to the fitting results of the 4D Q data. We obtain $T_c(\mathrm{XY}) = 3.314\,437(6)$, and in Fig. 2(a) we illustrate the location of T_c by Q.

We further examine the estimate of T_c by the FSS of other quantities, such as the magnetization density m. For the XY model, in Fig. 2(b) we give a log-log plot of the mL data versus $\ln L$ for $T = T_c$, as well as for $T_{\mathrm{low}} = 3.314\,40$ and $T_{\mathrm{above}} = 3.314\,50$. The significant bending-up and bending-down features clearly suggest that $T_{\mathrm{low}} < T_c$ and $T_{\mathrm{above}} > T_c$, providing confidence for the finally quoted error margin of T_c.

The final estimates of T_c are summarized in Table 1. For $n = 1$, we have $T_c = 6.680\,300(10)$, which is consonant with and improves over $T_c = 6.680\,263(23)$ [37] and marginally agrees with $T_c = 6.679\,63(36)$ [38] and $6.680\,339(14)$ [13]. For $n = 2$, our determination $T_c = 3.314\,437(6)$ significantly improves over $T_c = 3.31$ [39,40] and 3.314 [41]. For $n = 3$, our result $T_c = 2.198\,79(2)$ rules out $T_c = 2.192(1)$ from a high-temperature expansion [42].

Table 1. Estimates of T_c for the 4D O(n) vector models.

Model	T_c	Reference
Ising ($n = 1$)	6.679 63(36)	[38]
	6.680 339(14)	[13]
	6.680 263(23)	[37]
	6.680 300(10)	This work
XY ($n = 2$)	3.31 and 3.314	[39–41]
	3.314 437(6)	This work
Heisenberg ($n = 3$)	2.192(1)	[42]
	2.198 79(2)	This work

Finite-size scaling of the two-point correlation

We then fit the critical two-point correlation $g(L/2, L)$ to

$$g(L/2, L) = v_1 L^{-2} (\ln L)^{\hat{p}} + v_2 L^{-2}, \qquad (14)$$

where the first term comes from the large-distance plateau and the second term comes from the r-dependent behavior of $g(r, L)$. With $\hat{p} = 1/2$ being fixed, the estimate of the leading scaling term $L^{-1.98(4)}$ agrees well with the exact L^{-2}. With the exponent -2 in L^{-2} being fixed, the result $\hat{p} = 0.5(1)$ is also well consistent with the prediction $\hat{p} = 1/2$. These results are elaborated in the online supplementary material.

We remark that FSS analyses for $g(L/2, L)$ have already been performed in [16] with the formula $g(L/2, L) = AL^{-2}[\ln(L/2 + B)]^{1/2}$ (A and B are constants) and in [13] with a similar formula. These FSSs in the literature correspond to the first scaling term in (14). Hence, (14) serves as a forward step for complete FSS by involving the scaling term $v_2 L^{-2}$, which arises from the Gaussian fixed point.

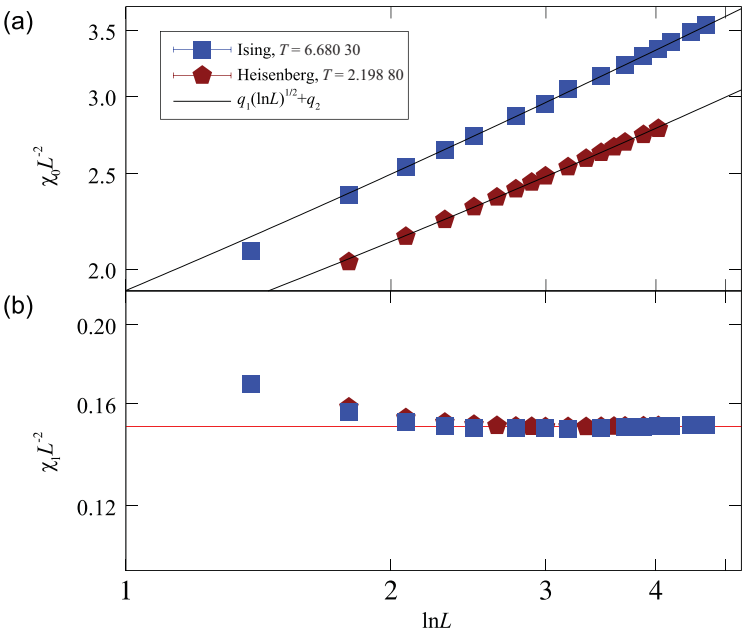

Figure 3. The magnetic fluctuations (a) χ_0 and (b) χ_1 rescaled by L^2 versus $\ln L$ on a log-log scale for the critical Ising and Heisenberg models. The black lines in (a) represent the least-squares fits, and the red line in (b) denotes a constant.

Finite-size scaling of the magnetic susceptibility

According to (11) and (12), we fit the critical susceptibility χ_0 to

$$\chi_0 = q_1 L^2 (\ln L)^{\hat{p}} + q_2 L^2 \qquad (15)$$

with q_1 and q_2 nonuniversal constants. For $\hat{p} = 1/2$ being fixed, we obtain fitting results with $\chi^2/\mathrm{DF} \lesssim 1$ for each $n = 1, 2, 3$, and correctly produce the leading scaling form L^2. The scaled susceptibility $\chi_0 L^{-2}$ versus $\ln L$ is shown in Fig. 1(c) for the XY model and in Fig. 3(a) for the Ising and Heisenberg models.

We note that previous studies based on a FSS without high-order corrections produced estimates of $\hat{y}_h$ ($= \hat{p}/2$), considered to be consistent with $\hat{y}_h = 1/4$ [38,43–45]. The maximum lattice size therein was $L_{\max} = 24$, four times smaller than $L_{\max} = 96$ of the present study. In particular, it was reported [43] that $2\hat{y}_h = 0.45(8)$ and $4\hat{y}_h = 0.80(25)$. Nevertheless, we find that the fit $\chi_0 = q_1 L^2 (\ln L)^{2\hat{y}_h}$ by dropping the correction term $q_2 L^2$ would yield $\hat{y}_h = 0.21(1)$ (Ising), $0.20(1)$ (XY), and $0.19(1)$ (Heisenberg), which are smaller than and inconsistent with the predicted value $\hat{y}_h = 1/4$. This suggests the significance of $q_2 L^2$ in the susceptibility χ_0, which arises from the r dependence of $g(r, L)$.

Finite-size scaling of the magnetic fluctuations at nonzero Fourier modes

We consider the magnetic fluctuations χ_1 with $|\mathbf{k}_1| = 2\pi/L$ and χ_2 with $|\mathbf{k}_2| = 2\sqrt{2}\pi/L$. We have compared the FSSs of χ_0, χ_1 and χ_2 in Fig. 1(c) and (d) for the critical 4D XY model. As L increases, $\chi_1 L^{-2}$ and $\chi_2 L^{-2}$ converge rapidly, suggesting the absence of a multiplicative logarithmic correction. This is in sharp contrast to the behavior of $\chi_0 L^{-2}$, which diverges logarithmically. For the Ising and Heisenberg models, the FSS of the fluctuations at nonzero modes is also free of a multiplicative logarithmic correction (Fig. 3(b)).

Surprisingly, we find that the scaled fluctuations $\chi_1 L^{-2} \approx 0.15$ are equal within error bars for the Ising, XY and Heisenberg models.

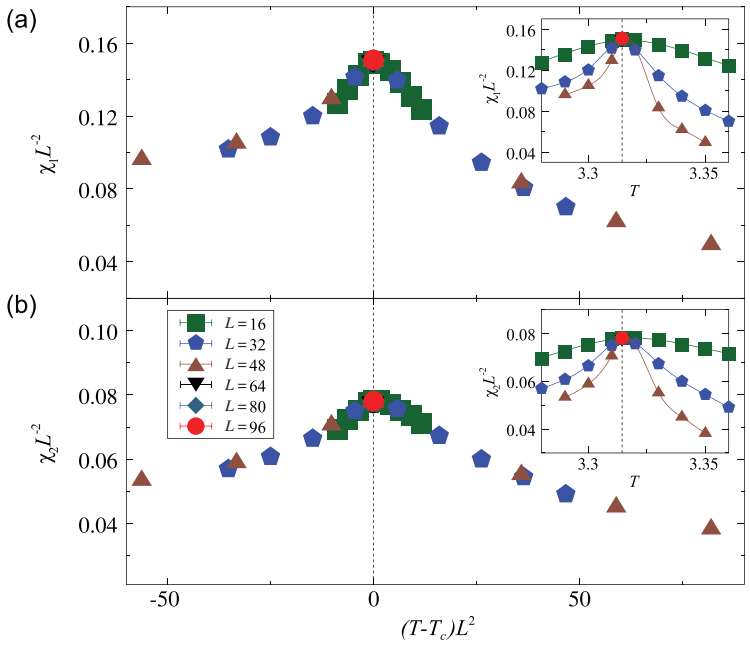

Figure 4. Data collapses for the magnetic fluctuations (a) χ_1 and (b) χ_2 rescaled by L^{2y_h-d} and L^{y_t} ($y_h=3$, $y_t=2$, $d=4$) for the 4D XY model. The insets show the scaled fluctuations versus T, and the dashed lines denote T_c.

Furthermore, we show in Fig. 4 χ_1 and χ_2 versus T for the 4D XY model. We observe that the magnetic fluctuations at nonzero Fourier modes reach maximum at T_c and that the $\chi_1 L^{-2}$ ($\chi_2 L^{-2}$) data for different Ls collapse well not only at T_c but also for a wide range of $(T-T_c)L^{y_t}$ with $y_t=2$.

DISCUSSIONS

We propose formulae (11) and (12) for the FSS of the O(n) universality class at the upper critical dimensionality, which are tested against extensive MC simulations with $n=1, 2, 3$. From the FSS of the magnetic fluctuations at zero and nonzero Fourier modes, the two-point correlation function and the Binder cumulant, we obtain complementary and solid evidence supporting (11) and (12). As byproducts, the critical temperatures for $n=1, 2, 3$ are all located up to an unprecedented precision.

An immediate application of (12) is to the massive amplitude excitation mode (often called the Anderson–Higgs boson) due to the spontaneous breaking of the continuous O(n) symmetry [46], which is at the frontier of condensed matter research. At the pressure-induced quantum critical point (QCP) in the dimerized quantum antiferromagnet $TlCuCl_3$, the 3D O(3) amplitude mode was probed by neutron spectroscopy and a rather narrow peak width of about 15% of the excitation energy was revealed, giving no evidence for the logarithmic reduction of the width-mass ratio [3]. This was later confirmed by a quantum MC study of a 3D model Hamiltonian of O(3) symmetry [5,6]. Indeed, (12) provides an explanation why the logarithmic-correction reduction in the Higgs resonance was not observed at the 3D QCP. In numerical studies of the Higgs excitation mode at the 3D QCP, the correlation function $g(\tau \equiv |\tau_1 - \tau_2|)$ is measured along the imaginary-time axis β, and numerical analytical continuation is used to deal with the $g(\tau)$ data. In practice, simulations are carried out at very low temperature $\beta \to \infty$, and it is expected that $g(\tau) \asymp \tau^{-2}$ for a significantly wide range of τ. Furthermore, it is the τ-dependent behavior of $g(\tau)$, instead of the L dependence, that plays a decisive role in numerical analytical continuation.

In the thermodynamic limit, the two-point correlation function decays as $g(r) \sim r^{-2}\tilde{g}(r/\xi)$, where the scaling function $\tilde{g}(r/\xi)$ quickly drops to zero as $r/\xi \gg 1$. It can be seen that no multiplicative logarithmic correction exists in the algebraic decaying behavior. On the other hand, as the criticality is approached ($t \to 0$), the correlation length diverges as $\xi(t) \sim t^{-1/2}|\ln t|^{\hat{\nu}}$, and $\hat{\nu} = (n+2)/2(n+8) > 0$ implies that ξ diverges faster than $t^{-1/2}$ [30,33]. Since the susceptibility can be calculated by summing the correlation as $\chi_0 \sim \int_0^{\xi} g(r) r^{d-1} dr \sim \xi^2$, we have $\chi_0(t) \sim t^{-1}|\ln t|^{\hat{\gamma}}$ with $\hat{\gamma} = 2\hat{\nu}$. The thermodynamic scaling of $\chi_0(t)$ can also be obtained from the FSS formula (10) or (11), which gives $\chi_0(t, L) \sim L^{2y_h-4}(\ln L)^{2\hat{y}_h}\tilde{\chi}_0(tL^{y_t}(\ln L)^{\hat{y}_t})$. By fixing $tL^{y_t}(\ln L)^{\hat{y}_t}$ at some constant, we obtain the relation $L \sim t^{-1/y_t}|\ln t|^{-\hat{y}_t/y_t}$. Substituting this into the FSS of $\chi_0(t, L)$ yields $\chi_0(t) \sim t^{\gamma}|\ln t|^{\hat{\gamma}}$ with $\gamma = (2y_h-4)/y_t$ and $\hat{\gamma} = -\gamma\hat{y}_t + 2\hat{y}_h$. With $(y_t, y_h, \hat{y}_t, \hat{y}_h) = (2, 3, (4-n)/(2n+16), \frac{1}{4})$, we have $\gamma = 1$ and $\hat{\gamma} = (n+2)/(n+8)$. The thermodynamic scaling with logarithmic corrections has been demonstrated in [4] in terms of the magnetization m of an O(3) Hamiltonian.

For the critical Ising model in five dimensions, an unwrapped distance r_u was introduced to account for the winding numbers across a finite torus [18]. The unwrapped correlation was shown to behave as $g(r_u) \sim r_u^{2-d}\tilde{g}(r_u/\xi_u)$, where the unwrapped correlation length diverges as $\xi_u \sim L^{d/4}$. This differs from typical correlation functions that are cut off by a linear system size of approximately L. We expect that at $d_c = 4$ the unwrapped correlation length diverges as $\xi_u \sim L(\ln L)^{\hat{y}_h}$, which gives the critical susceptibility as $\chi_0(L) \sim L^2(\ln L)^{2\hat{y}_h}$.

Besides, (12) is useful for predicting various critical behaviors. As an instance, it was observed that an impurity immersed in a 2D O(2) quantum critical environment can evolve into a quasiparticle of fractionalized charge, as the impurity-environment interaction is tuned to a

boundary critical point [47–49]. Equation (12) precludes the emergence of such a quantum-fluctuation-induced quasiparticle at the 3D O(2) QCP.

We mention an open question about the specific heat of the 4D Ising model. The FSS formula (10) predicts that the critical specific heat diverges as $C \asymp (\ln L)^{1/3}$. By contrast, an MC study demonstrated that the critical specific heat is bounded [37]. The complete scaling form (11) is potentially useful for reconciling the inconsistency.

Finally, it would be possible to extend the present scheme to other systems of critical phenomena, as the existence of upper critical dimensionality is a common feature therein. These systems include the percolation and spin-glass models at their upper critical dimensionality $d_c = 6$. We leave this for a future study.

METHODS

Throughout the paper, the raw data for any temperature T and linear size L are obtained by means of MC simulations, for which the Wolff cluster algorithm [35] and the Prokof'ev–Svistunov worm algorithm [36] are employed complementarily. Both algorithms are state-of-the-art tools in their own territories.

The O(n) vector model (1) in its original spin representation is efficiently sampled by the Wolff cluster algorithm, which is the single-cluster version of the widely utilized nonlocal cluster algorithms. The present study uses the standard procedure of the algorithm, as in the original paper [35] where the algorithm was invented. In some situations, we also use the conventional Metropolis algorithm [50] for benchmarks. The macroscopic physical quantities of interest have been introduced in aforementioned sections for the spin representation.

The two-point correlation function for the XY model ($n = 2$) is sampled by means of the Prokof'ev–Svistunov worm algorithm, which was invented for a variety of classical statistical models [36]. By means of a high-temperature expansion, we perform an exact transformation for the original XY spin model to a graphic model in directed-flow representation. We then introduce two defects for enlarging the state space of directed flows. The Markov chain process of evolution is built upon biased random walks of defects, which satisfy the detailed balance condition. It is defined that the evolution hits the original directed-flow state space when the two defects meet at a site. The details for the exact transformation and a step-by-step procedure for the algorithm have been presented in [51].

SUPPLEMENTARY DATA

Supplementary data are available at *NSR* online.

ACKNOWLEDGEMENTS

Y.D. is indebted to valuable discussions with Timothy Garoni, Jens Grimm and Zongzheng Zhou.

FUNDING

This work was supported by the National Natural Science Foundation of China (11774002, 11625522 and 11975024), the National Key R&D Program of China (2016YFA0301604 and 2018YFA0306501), and the Department of Education in Anhui Province.

AUTHOR CONTRIBUTIONS

J.-P.L., K.C. and Y.D. designed the research and established the formulae for finite-size scaling. J.-P.L., W.X. and Y.S. performed the simulations. J.-P.L., W.X., Y.S. and Y. D. analyzed the results. J.-P.L. and Y.D. wrote the manuscript. All the authors participated in the revisions of the manuscript.

Conflict of interest statement. None declared.

REFERENCES

1. Fernández R, Fröhlich J and Sokal AD. *Random Walks, Critical Phenomena, and Triviality in Quantum Field Theory*. Berlin: Springer, 2013.
2. Svistunov BV, Babaev ES and Prokof'ev NV. *Superfluid States of Matter*. London: CRC Press, 2015.
3. Merchant P, Normand B and Krämer KW *et al.* Quantum and classical criticality in a dimerized quantum antiferromagnet. *Nat Phys* 2014; **10**: 373–9.
4. Qin YQ, Normand B and Sandvik AW *et al.* Multiplicative logarithmic corrections to quantum criticality in three-dimensional dimerized antiferromagnets. *Phys Rev B* 2015; **92**: 214401.
5. Lohöfer M and Wessel S. Excitation-gap scaling near quantum critical three-dimensional antiferromagnets. *Phys Rev Lett* 2017; **118**: 147206.
6. Qin YQ, Normand B and Sandvik AW *et al.* Amplitude mode in three-dimensional dimerized antiferromagnets. *Phys Rev Lett* 2017; **118**: 147207.
7. Cui Y, Zou H and Xi N *et al.* Quantum criticality of the Ising-like screw chain antiferromagnet $SrCo_2V_2O_8$ in a Transverse magnetic field. *Phys Rev Lett* 2019; **123**: 067203.
8. Resnick DJ, Garland JC and Boyd JT *et al.* Kosterlitz-Thouless transition in proximity-coupled superconducting arrays. *Phys Rev Lett* 1981; **47**: 1542–5.
9. Goldman A. *Percolation, Localization, and Superconductivity*, Vol. 109. Boston: Springer, 2013.
10. Greiner M, Mandel O and Esslinger T *et al.* Quantum phase transition from a superfluid to a Mott insulator in a gas of ultracold atoms. *Nature* 2002; **415**: 39–44.

11. Capogrosso-Sansone B, Prokof'ev NV and Svistunov BV. Phase diagram and thermodynamics of the three-dimensional Bose-Hubbard model. *Phys Rev B* 2007; **75**: 134302.
12. Cardy J. *Finite-Size Scaling, Vol. 2*. Amsterdam: Elsevier, 2012.
13. Luijten E. *Interaction Range, Universality and the Upper Critical Dimension*. Delft: Delft University Press, 1997.
14. Luijten E, Binder K and Blöte HWJ. Finite-size scaling above the upper critical dimension revisited: the case of the five-dimensional Ising model. *Euro Phys J B* 1999; **9**: 289–97.
15. Wittmann M and Young AP. Finite-size scaling above the upper critical dimension. *Phys Rev E* 2014; **90**: 062137.
16. Kenna R and Berche B. Fisher's scaling relation above the upper critical dimension. *Europhys Lett* 2014; **105**: 26005.
17. Flores-Sola E, Berche B and Kenna R *et al*. Role of Fourier modes in finite-size scaling above the upper critical dimension. *Phys Rev Lett* 2016; **116**: 115701.
18. Grimm J, Elçi EM and Zhou Z *et al*. Geometric explanation of anomalous finite-size scaling in high dimensions. *Phys Rev Lett* 2017; **118**: 115701.
19. Papathanakos V. Finite-size effects in high-dimensional statistical mechanical systems: the Ising model with periodic boundary conditions. *Ph.D. Thesis*. Princeton University, 2006.
20. Zhou Z, Grimm J and Fang S *et al*. Random-length random walks and finite-size scaling in high dimensions. *Phys Rev Lett* 2018; **121**: 185701.
21. Fang S, Grimm J and Zhou Z *et al*. Complete graph and Gaussian fixed point asymptotics in the five-dimensional Fortuin-Kasteleyn Ising model with periodic boundaries. *Phys Rev E* 2020; **102**: 022125.
22. Fisher ME. Critical phenomena. In: Green MS (ed.). *Proceedings of the 51st Enrico Fermi Summer School*. New York: Academic, 1971.
23. Binder K, Nauenberg M and Privman V *et al*. Finite-size tests of hyperscaling. *Phys Rev B* 1985; **31**: 1498–502.
24. Berche B, Kenna R and Walter JC. Hyperscaling above the upper critical dimension. *Nucl Phys B* 2012; **865**: 115–32.
25. Kenna R and Berche B. A new critical exponent koppa and its logarithmic counterpart koppa-hat. *Cond Matt Phys* 2013; **16**: 23601.
26. Aizenman M. Geometric analysis of φ^4 fields and Ising models. Parts I and II. *Commun Math Phys* 1982; **86**: 1–48.
27. Aizenman M. Rigorous studies of critical behavior II. In: Fritz J, Jaffe A and Szasz D (eds). *Statistical Physics and Dynamical Systems: Rigorous Results*. Boston: Birkhauser, 1985, 453–81.
28. Aizenman M. Rigorous studies of critical behavior. *Physica A* 1986; **140**: 225–31.
29. Huang W, Hou P and Wang J *et al*. Critical percolation clusters in seven dimensions and on a complete graph. *Phys Rev E* 2018; **97**: 022107.
30. Kenna R. Finite size scaling for O(N) ϕ^4-theory at the upper critical dimension. *Nucl Phys B* 2004; **691**: 292–304.
31. Aktekin N. The finite-size scaling functions of the four-dimensional Ising model. *J Stat Phys* 2001; **104**: 1397–406.
32. Wegner FJ and Riedel EK. Logarithmic corrections to the molecular-field behavior of critical and tricritical systems. *Phys Rev B* 1973; **7**: 248.
33. Kenna R. Universal scaling relations for logarithmic-correction exponents. In: Holovatch Y (ed.). *Order, Disorder and Criticality, Advanced Problems of Phase Transition Theory*. New York: World Scientific, 2012.
34. Slade G and Tomberg A. Critical correlation functions for the 4-dimensional weakly self-avoiding walk and n-component ϕ^4 model. *Commun Math Phys* 2016; **342**: 675–737.
35. Wolff U. Collective Monte Carlo updating for spin systems. *Phys Rev Lett* 1989; **62**: 361.
36. Prokof'ev NV and Svistunov BV. Worm algorithms for classical statistical models. *Phys Rev Lett* 2001; **87**: 160601.
37. Lundow PH and Markström K. Critical behavior of the Ising model on the four-dimensional cubic lattice. *Phys Rev E* 2009; **80**: 031104.
38. Kenna R and Lang CB. Finite size scaling and the zeroes of the partition function in the ϕ^4_4 model. *Phys Lett B* 1991; **264**: 396–400.
39. Jensen LM, Kim BJ and Minnhagen P. Critical dynamics of the four-dimensional XY model. *Physica B* 2000; **284**: 455–6.
40. Jensen LM, Kim BJ and Minnhagen P. Dynamic critical exponent of two-, three-, and four-dimensional XY models with relaxational and resistively shunted junction dynamics. *Phys Rev B* 2000; **61**: 15412.
41. Nonomura Y and Tomita Y. Critical nonequilibrium relaxation in the Swendsen-Wang algorithm in the Berezinsky-Kosterlitz-Thouless and weak first-order phase transitions. *Phys Rev E* 2015; **92**: 062121.
42. McKenzie S, Domb C and Hunter DL. The high-temperature susceptibility of the classical Heisenberg model in four dimensions. *J Phys A Math Gen* 1982; **15**: 3909–14.
43. Lai PY and Mon KK. Finite-size scaling of the Ising model in four dimensions. *Phys Rev B* 1990; **41**: 9257–63.
44. Kenna R and Lang CB. Renormalization group analysis of finite-size scaling in the ϕ^4_4 model. *Nucl Phys B* 1993; **393**: 461–79.
45. Kenna R and Lang CB. Scaling and density of Lee-Yang zeros in the four-dimensional Ising model. *Phys Rev E* 1994; **49**: 5012.
46. Pekker D and Varma CM. Amplitude/Higgs modes in condensed matter physics. *Annu Rev Condens Matter Phys* 2015; **6**: 269–97.
47. Huang Y, Chen K and Deng Y *et al*. Trapping centers at the superfluid–Mott-insulator criticality: transition between charge-quantized states. *Phys Rev B* 2016; **94**: 220502.
48. Whitsitt S and Sachdev S. Critical behavior of an impurity at the boson superfluid–Mott-insulator transition. *Phys Rev A* 2017; **96**: 053620.
49. Chen K, Huang Y and Deng Y *et al*. Halon: a quasiparticle featuring critical charge fractionalization. *Phys Rev B* 2018; **98**: 214516.
50. Metropolis N, Rosenbluth AW and Rosenbluth MN *et al*. Equation of state calculations by fast computing machines. *J Chem Phys* 1953; **21**: 1087–92.
51. Xu W, Sun Y and Lv JP *et al*. High-precision Monte Carlo study of several models in the three-dimensional U(1) universality class. *Phys Rev B* 2019; **100**: 064525.